Long-term stable, sub-femtosecond timing distribution via a 1.2-km polarization-maintaining fiber link: approaching 10^{-21} link stability

Michael Y. Peng,[1,*] Patrick T. Callahan,[1] Amir H. Nejadmalayeri,[1] Stefano Valente,[2,3] Ming Xin,[2] Lars Grüner-Nielsen,[4] Eric M. Monberg,[5] Man Yan,[5] John M. Fini,[5] and Franz X. Kärtner[1,2,6]

[1]*Department of Electrical Engineering and Computer Science and Research Laboratory for Electronics, Massachusetts Institute of Technology, 77 Massachusetts Avenue, Cambridge, Massachusetts 02139, USA*
[2]*Center for Free-Electron Laser Science, Deutsches Elektronen-Synchrotron, Luruper Chaussee 149, Hamburg 22761, Germany*
[3]*Department of Electrical Engineering and Computer Science, University of L'Aquila, Via Campo di Pile - Zona industriale di Pile, 67100 L'Aquila, Italy*
[4]*OFS, Priorparken 680, 2605 Brondby, Denmark*
[5]*OFS Laboratories, 25 Schoolhouse Road, Somerset, New Jersey 08873, USA*
[6]*Department of Physics, University of Hamburg, Notkestraße 85, Hamburg 22607, Germany*
[*]*mypeng@mit.edu*

Abstract: Long-term stable, sub-femtosecond timing distribution over a 1.2-km polarization-maintaining (PM) fiber-optic link using balanced optical cross-correlators for link stabilization is demonstrated. Novel dispersion-compensating PM fiber was developed to construct a dispersion-slope-compensated PM link, which eliminated slow timing drifts and jumps previously induced by polarization mode dispersion in standard single-mode fiber. Numerical simulations of nonlinear pulse propagation in the fiber link confirmed potential sub-100-as timing stability for pulse energies below 70 pJ. Link operation for 16 days showed ~0.6 fs RMS timing drift and during a 3-day interval only ~0.13 fs drift, which corresponds to a stability level of 10^{-21}.

OCIS codes: (060.2360) Fiber optics links and subsystems; (060.2420) Fibers, polarization-maintaining; (320.7160) Ultrafast technology; (120.7000) Transmission; (120.4825) Optical time domain reflectometry; (060.5530) Pulse propagation and temporal solitons.

References and links

1. P. Emma, R. Akre, J. Arthur, R. Bionta, C. Bostedt, J. Bozek, A. Brachmann, P. Bucksbaum, R. Coffee, F.-J. Decker, Y. Ding, D. Dowell, S. Edstrom, A. Fisher, J. Frisch, S. Gilevich, J. Hastings, G. Hays, P. Hering, Z. Huang, R. Iverson, H. Loos, M. Messerschmidt, A. Miahnahri, S. Moeller, H.-D. Nuhn, G. Pile, D. Ratner, J. Rzepiela, D. Schultz, T. Smith, P. Stefan, H. Tompkins, J. Turner, J. Welch, W. White, J. Wu, G. Yocky, and J. Galayda, "First lasing and operation of an ångstrom-wavelength free-electron laser," Nat. Photonics **4**(9), 641–647 (2010).
2. M. Altarelli, R. Brinkmann, M. Chergui, W. Decking, B. Dobson, S. Düsterer, G. Grübel, W. Graeff, H. Graafsma, and J. Hajdu, *XFEL: The European X-Ray Free-Electron Laser. Technical Design Report* (DESY, 2006).
3. C. J. Bocchetta and G. De Ninno, *FERMI@ Elettra: Conceptual Design Report* (Sincrotrone, 2007).
4. J. M. Byrd, L. Doolittle, G. Huang, J. W. Staples, R. B. Wilcox, J. Arthur, J. C. Frisch, and W. E. White, "Femtosecond synchronization of laser systems for the LCLS," in *Proceedings of International Particle Accelerator Conference* (2010), 58–60.
5. J. Kim, J. A. Cox, J. Chen, and F. X. Kärtner, "Drift-free femtosecond timing synchronization of remote optical and microwave sources," Nat. Photonics **2**(12), 733–736 (2008).
6. Y. Ding, F.-J. Decker, P. Emma, C. Feng, C. Field, J. Frisch, Z. Huang, J. Krzywinski, H. Loos, J. Welch, J. Wu, and F. Zhou, "Femtosecond X-Ray Pulse Characterization in Free-Electron Lasers Using a Cross-Correlation Technique," Phys. Rev. Lett. **109**(25), 254802 (2012).
7. H. A. Haus and A. Mecozzi, "Noise of mode-locked lasers," IEEE J. Quantum Electron. **29**(3), 983–996 (1993).

#192815 - $15.00 USD Received 26 Jun 2013; revised 12 Aug 2013; accepted 12 Aug 2013; published 16 Aug 2013

8. J. Kim, J. Chen, J. Cox, and F. X. Kärtner, "Attosecond-resolution timing jitter characterization of free-running mode-locked lasers," Opt. Lett. **32**(24), 3519–3521 (2007).
9. J. Kim, J. Chen, Z. Zhang, F. N. C. Wong, F. X. Kärtner, F. Loehl, and H. Schlarb, "Long-term femtosecond timing link stabilization using a single-crystal balanced cross correlator," Opt. Lett. **32**(9), 1044–1046 (2007).
10. J. Kim and F. X. Kärtner, "Attosecond-precision ultrafast photonics," Laser Photonics Rev. **4**(3), 432–456 (2010).
11. M. Ferianis, A. Borga, A. Bucconi, L. Pavlovic, M. Predonzani, and F. Rossi, "All-Optical Femtosecond Timing System for the Fermi@ Elettra FEL," in *Proceedings of Free Electron Laser Conference* (2011), 641–647.
12. J. A. Cox, "Sub-femtosecond precision timing distribution, synchronization and coherent synthesis of ultrafast lasers," Thesis, Massachusetts Institute of Technology (2012).
13. A. H. Nejadmalayeri, F. N. C. Wong, T. D. Roberts, P. Battle, and F. X. Kärtner, "Guided wave optics in periodically poled KTP: quadratic nonlinearity and prospects for attosecond jitter characterization," Opt. Lett. **34**(16), 2522–2524 (2009).
14. M. Ferianis, "State of the art in high-stability timing, phase reference distribution and synchronization systems," in *Proceedings of Particle Accelerator Conference* (2009), 1915–1919.
15. M. Y. Peng, P. T. Callahan, A. H. Nejadmalayeri, S. Valente, K. Ahmed, M. Xin, E. Monberg, M. Yan, L. Grüner-Nielsen, J. M. Fini, T. D. Roberts, P. Battle, and F. X. Kärtner, "Towards a large-scale, optical timing distribution system with sub-femtosecond residual timing jitter," in *Proceedings of IEEE International Frequency Control Symposium* (2013).
16. G. Agrawal, *Nonlinear Fiber Optics* (Academic Press, 2012).

1. Introduction

Modern large-scale scientific facilities such as X-ray free-electron lasers (FELs) [1–3] require timing distribution systems with extremely high timing stability to synchronize RF and optical sources across hundreds of meters to several kilometers. Since conventional RF timing systems have already reached a practical limit for timing precision of about 50-100 fs for such long distances, next-generation timing systems are adopting fiber-optic technology to achieve superior performance with optical signal transport and timing distribution. Optical timing systems based on continuous-wave [4] and pulsed [5] operation have been explored and implemented successfully in select facilities to provide sub-10-fs timing stability.

Over the past decade, we have been advancing technology for a pulsed optical timing distribution system [5]. Our system consists of a femtosecond mode-locked laser tightly locked to a microwave standard and stabilized fiber links for distributing the pulsed optical timing signals to remote locations. Link stabilization is performed using compact, single-crystal balanced optical cross-correlators (BOCs), which are capable of attosecond-level timing resolution. Our previous results with a 300-m stabilized fiber link using standard single-mode fiber showed that polarization mode dispersion (PMD) limited the link stability to about 10 fs over few days of operation and caused delay jumps as much as 100 fs when the fiber was significantly perturbed.

In the near future, sub-fs timing stability will be demanded; current FELs can already produce sub-10-fs X-ray pulses [6] and concepts for sub-fs X-ray pulse generation are in place. Improving upon our previous work, we demonstrate here long-term stabilization of a 1.2-km polarization-maintaining (PM), dispersion-compensated fiber link with sub-fs residual timing drift over 16 days of uninterrupted operation.

2. Principle of operation

The principle of operation of our timing-stabilized link is shown in Fig. 1. The timing signal, which is an ultralow-noise optical pulse train generated from a mode-locked laser [7], is distributed between two remote locations through a dispersion-slope-compensated PM fiber link. The master laser may be locked to a microwave standard to improve the low-frequency noise of the timing signal. Link stabilization requires maintaining a constant time-of-flight for pulses from the link input to the link output. When the link is not stabilized, slow fiber fluctuations due to thermal, acoustic, and mechanical disturbances will induce timing errors in the output pulse arrival times. For example, ambient temperature fluctuations of 1 K for a 1.2-km fiber link with a thermal expansion coefficient of 5×10^{-7} cm/cm·K will induce length changes equivalent to picoseconds of timing error.

Our link stabilization scheme begins with detecting the round-trip timing error. The output coupler at the end of the link partially reflects the output pulse back to the input. A BOC then

#192815 - $15.00 USD Received 26 Jun 2013; revised 12 Aug 2013; accepted 12 Aug 2013; published 16 Aug 2013

measures the difference in arrival times, Δt, between the round-trip pulse and a new laser pulse and outputs a corresponding error voltage, $V = K_s \cdot \Delta t$, where K_s is the BOC timing sensitivity. The BOC is based on balanced detection of a double-pass, type-II phase-matched second harmonic generation in a periodically-poled $KTiOPO_4$ (PPKTP) crystal and is capable of as-level timing resolution [8]. With proper locking electronics, the error voltage is fed back to a variable delay in the link to correct for the detected timing errors. The feedback will force the error voltage to zero by suppressing slow fluctuations within the loop bandwidth, thus achieving long-term timing stabilization. Output pulses of the stabilized link can then proceed to remote optical-to-optical and optical-to-RF synchronization.

Note that since the variable delay works bidirectionally, the timing errors acquired during the forward- and reverse-pass must be equal; otherwise, eliminating the round-trip timing error will still result in a timing error at the link output. Therefore, only timing fluctuations that occur on a timescale slower than the round-trip propagation time can be compensated.

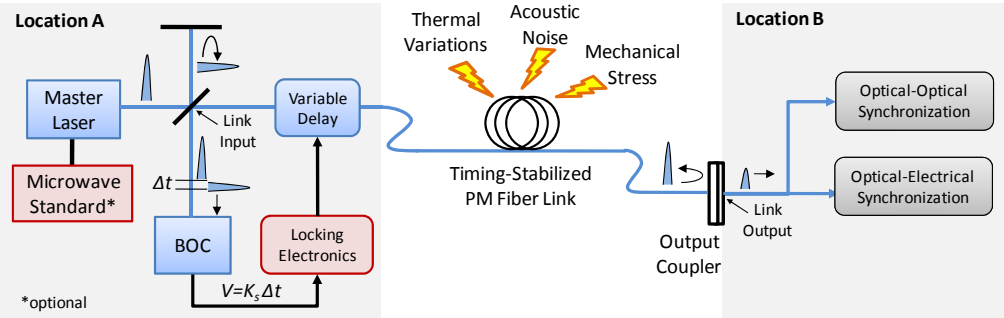

Fig. 1. General schematic of the timing-stabilized PM fiber link. Pulse timing error, Δt, acquired during round-trip propagation in the fiber link is measured with a balanced optical cross-correlator (BOC) and corrected for by a variable delay operated under negative feedback.

3. System demonstration

3.1 Experimental set-up

The experimental set-up of the 1.2-km timing-stabilized PM link is shown in Fig. 2. The mode-locked laser is a free-running Er-doped fiber laser (Menlo Systems, M-Comb-Custom) that outputs 170-fs pulses centered at 1557.66 nm with + 20 dBm average power and a 200-MHz fundamental repetition rate. The pulse width and repetition rate are selected to keep higher-order dispersion and nonlinear fiber effects low. The set-up is divided into two sections: the in-loop section, which performs link stabilization, and the out-of-loop cross-correlator, which evaluates the link stability relative to the input pulse stream.

In the in-loop section, the pulses are divided into reference and signal pulses. The reference pulses serve as a timing reference for the in-loop BOC. The signal pulses are transmitted through the link, which consists of a voltage-controlled variable delay line, 45° Faraday rotator, half-wave plate, 1.2-km PM link, and a 10% output coupler. Since pulse propagation is restricted to a single axis in the PM link, the 45° Faraday rotator is necessary to induce a 90° round-trip polarization rotation so that the returning link pulses will reach the in-loop BOC. The half-wave plate aligns the input polarization with the slow axis of the PM link. The power coupled into the PM link input was + 11 dBm, which is near the onset of fiber nonlinearities. With 10% output coupling, the reflected power was sufficient for link stabilization without an optical amplifier.

The 1.2-km PM link, which was fabricated by OFS, consists of 1088 m of standard TruePhase PM fiber matched to 190 m of custom dispersion-compensating PM fiber (PM-DCF). The PM-DCF has a PANDA-like geometry containing Boron stress rods with 35-μm diameters and a core index profile similar to conventional DCF. It has a measured birefringence of 2.9×10^{-4}, loss of 0.42 dB/km, wavelength cut-off at 1520 nm, and

#192815 - $15.00 USD Received 26 Jun 2013; revised 12 Aug 2013; accepted 12 Aug 2013; published 16 Aug 2013

dispersion and dispersion slope of −104.1 ps/nm·km and −0.34 ps/nm^2·km, respectively, at 1550 nm for the slow axis. To minimize losses, the small-mode-size (A_{eff} = 22 μm^2) PM-DCF was spliced to an intermediate bridge fiber before splicing to standard PM fiber. For a single-pass through the link, the loss is 2.7 dB and the polarization extinction ratio is >20 dB. For operation near 1557.66 nm, the residual link dispersion was compensated by adding 2.4 m of standard PM fiber to achieve a minimum pulse width of 250 fs at the link output.

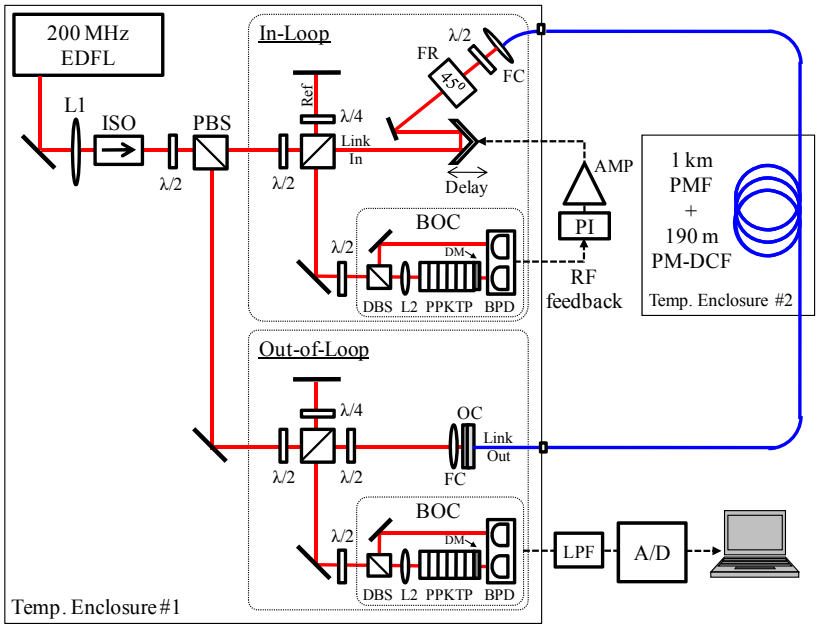

Fig. 2. Schematic of the experimental set-up for the timing-stabilized 1.2-km PM fiber link; EDFL, Erbium-doped fiber laser; L1, collimator; ISO, isolator; λ/2, half-wave plate; λ/4, quarter-wave plate; PBS, polarizing beam-splitter; FR, 45° Faraday rotator; FC, fiber collimator; PMF, standard PM fiber; PM-DCF, dispersion-compensating PM fiber; OC, output coupler; BOC, balanced optical cross-correlator; DBS, dichroic beam-splitter; L2, focusing lens; PPKTP, periodically-poled $KTiOPO_4$; DM, dichroic mirror; BPD, balanced photodetector; PI, proportional-integral controller; AMP, high voltage amplifier; LPF, low-pass filter; A/D, analog-to-digital converter.

The stabilization feedback loop begins with the in-loop BOC, which consists of a single 4-mm PPKTP crystal operated in a double-pass configuration with appropriate dichroic elements [9]. The round-trip timing error is measured with a BOC timing sensitivity of 20 mV/fs. The locking electronics consists of a PI controller (Menlo Systems, PIC210), high voltage amplifier (Menlo Systems, HVA150) and a voltage-controlled variable delay built from mounting a retroreflector on a stacked combination of a 40-μm piezoelectric actuator (Thorlabs, PAS009) and a 25-mm motorized translation stage (PI, M-112.12S) for short- and long-term stabilization, respectively. The feedback loop bandwidth was 20 Hz.

Once the link stabilization is engaged, uncompensated timing errors will cause a timing drift at the link output. The out-of-loop BOC monitors this drift by measuring the timing error between the link output pulses and reference pulses. The BOC timing sensitivity is 3.5 mV/fs. For long-term link drift measurements, the out-of-loop BOC voltage is logged using an A/D converter at a 1-Hz sampling rate. The motor stage delay is also logged simultaneously to monitor the timing error compensated by the in-loop stabilization.

The link set-up was optimized to demonstrate the suppression of PMD-induced timing drifts, which occur on timescales slower than 1 Hz. Most of the optical power was allocated to the in-loop link stabilization to achieve the tightest locking possible. The remaining power was used by the out-of-loop BOC to observe low-frequency timing drifts. High-frequency link noise was obscured by the electronic noise floor of the balanced detector. Since we are

#192815 - $15.00 USD Received 26 Jun 2013; revised 12 Aug 2013; accepted 12 Aug 2013; published 16 Aug 2013

reporting here only long-term stability below 1 Hz, we used a 0.5-Hz low-pass filter after detection to improve the signal-to-noise ratio for our long-term drift measurement. Future work will include an intra-link fiber amplifier to allow direct monitoring of the high-frequency noise to evaluate short-term stability. Such a scheme has already been investigated and shown to reliably suppress high-frequency link noise below 1 fs RMS jitter [10].

Temperature stabilization and vibration isolation of the free-space optics are critical for sub-fs-level stability. Enclosures were built separately for the free-space optics and PM link. Each consisted of an external 2" layer of extruded polystyrene insulation foam and an internal Aluminum enclosure, which was temperature controlled with a resistive heater pad and PID controller. Lead foam was placed beneath the set-up to dampen vibrations from the table. Thermal fluctuations in free-space set-up were further reduced by minimizing differential optical path lengths and the number of kinematic mounts. The free-space enclosure had a constant setpoint of 27°C. The PM link temperature was set to a nominal value of 27°C and modulated with a peak deviation of ~0.05°C with a period of 20 min; this modulation allowed direct measurement of timing error due to thermal expansion in the fiber link.

3.2 Results and discussion

Sub-femtosecond timing stabilization of the 1.2-km PM link was achieved for 16 days without interruption. Recorded data for the link drift and motor delay are shown in Fig. 3(a). Although the data log for the motor delay faulted in day 13, the link stabilization remained unaffected. Overall, the motor delay corrected for over 65 ps of timing fluctuations. The remaining timing drift at the link output showed only a maximum deviation of 2.5 fs and a RMS value of 0.6 fs. This represents a suppression of timing fluctuations by a factor of more than 20,000 for 16 days of continuous operation, indicating that the PM fiber was effective in overcoming the previous 10-fs-level stability limit over few days of operation and eliminating large 100-fs delay jumps caused by PMD.

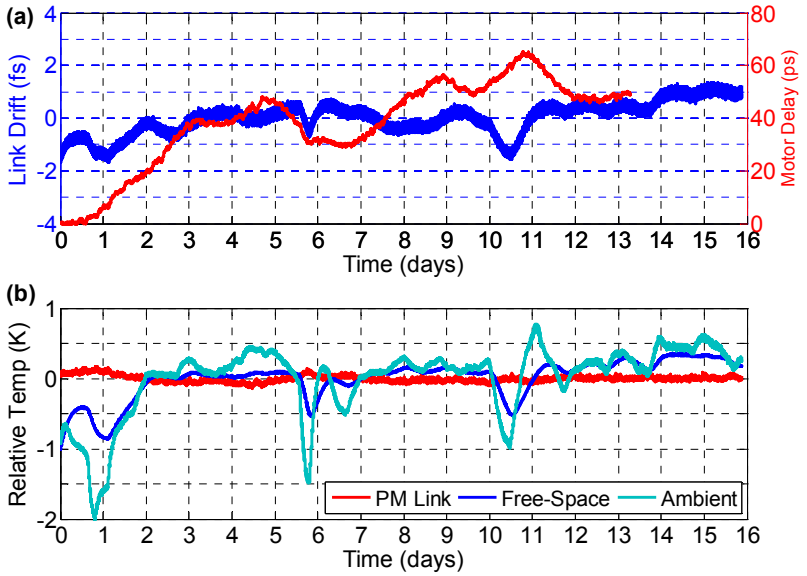

Fig. 3. Long-term measurements for the timing-stabilized 1.2-km PM fiber link over 16 days of continuous operation; (a) link drift, as measured by the out-of-loop BOC, and time delay, as controlled by the in-loop motor stage; (b) relative changes in the internal temperatures for the PM link and free-space enclosures and ambient temperature.

The current limitation for achieving sub-100-as stability is environmental fluctuations in the free-space set-up. Recorded data for relative changes in the internal temperatures of the PM link and free-space enclosures and ambient temperature are plotted in Fig. 3(b). The

#192815 - $15.00 USD Received 26 Jun 2013; revised 12 Aug 2013; accepted 12 Aug 2013; published 16 Aug 2013

strong correlation between the link drift, free-space enclosure temperature, and ambient temperature over the 16-day operation confirms that the link drift is limited by thermal fluctuations penetrating into the free-space set-up. This is reasonable because the free-space enclosure is large in volume, making it difficult to isolate the enclosed optics from the environment. In free-space, 1 fs of timing error is equal to a length change of only 0.3 μm. It is therefore highly probable that length changes on this scale are occurring between the in-loop and out-of-loop sections and are being falsely detected as link drift. Link drift is also sensitive to mechanical stress in the optical breadboard; slight pressure along one edge of the breadboard due to tension in power cables can result in a slow linear drift of 3 fs for over two weeks. Resolving these temperature and mechanical issues in the free-space set-up should yield 100-as-level stability or even better. This is evident during days 11-14 when ambient fluctuations were minimal, resulting in a RMS timing drift of only 0.13 fs.

In contrast to the free-space section, link stability is robust against temperature fluctuations introduced in the fiber link. A ~0.05°C modulation of the link temperature induced timing errors less than 1 ps. Scaling to current FEL facilities where ± 0.5°C stability is typically maintained [11], the expected 10-ps-level timing errors can be easily compensated. Robustness to high-frequency noise (e.g. acoustical and mechanical vibrations) requires further investigation and field testing.

As mentioned previously, our link configuration is sub-optimal due to limited laser power. One solution is to use an intra-link fiber amplifier; the required link input power can be reduced to increase the reference power for the BOCs. Timing sensitivities higher than 50 mV/fs [12] can be achieved to improve signal-to-noise ratios at detection and feedback stabilization. A more promising approach is to develop a fiber-coupled, all-integrated PPKTP BOC [13], which offers higher timing sensitivities at lower power levels compared to bulk-crystal BOCs. Since all other system components are already commercially available in fiber-coupled form, switching to an all-fiber implementation will greatly improve the temperature and mechanical stability.

In a complete timing distribution and synchronization system, the type of timing extraction method employed at the link output will determine the noise requirement for the master laser. The most stringent method requires an ultralow-noise master laser whose integrated phase noise for frequencies higher than the inverse of the desired time window [14] is in the sub-fs regime. The measured timing jitter of our current laser for the frequencies above 100 kHz has an upper limit of 1 fs [8], which may be too high for certain timing extraction methods. As a suitable replacement, we have characterized the jitter of two identical, commercially-available femtosecond lasers (OneFive, ORIGAMI) and confirmed that their timing jitter for frequencies higher than 1 kHz is less than 70 as and for 10 kHz is even less than 15 as [15], which would enable sub-100-as timing.

4. Nonlinearity-induced timing errors

Assuming that the issues with the environmental fluctuations in the free-space optics can be solved completely, we proceeded to assess the performance limit of pulsed optical timing distribution via fiber. Numerical simulations were performed to calculate the deterministic timing errors induced exclusively by fiber nonlinearities. These results allowed us to then calculate link timing drifts as a function of pulse energy fluctuations and to quantify an energy threshold over which nonlinearity-induced timing errors dominate.

The split-step Fourier method was used to simulate nonlinear pulse propagation through the 1.2-km PM link in the presence of real losses, 2nd- and 3rd-order dispersion, self-phase modulation (SPM), stimulated Raman scattering (SRS), and self-steepening [16]. At the link input, transform-limited 170-fs pulses centered at 1557.66 nm were linearly polarized and aligned with the slow axis of the PM link. Birefringence and PMD were ignored. After single-pass and round-trip propagation, the distorted pulses were cross-correlated with clean reference pulses using the thin-crystal BOC approximation [12] and normalized to generate the output voltage curves for the out-of-loop and in-loop BOCs, respectively (Fig. 4(a-b)).

#192815 - $15.00 USD Received 26 Jun 2013; revised 12 Aug 2013; accepted 12 Aug 2013; published 16 Aug 2013

The differential group delay was set to maximize the BOC sensitivity for the cross-correlation of two reference pulses. The simulation was repeated for pulse energies from 1 fJ to 110 pJ.

Although increasing the pulse energy generally steepens the zero-crossing slope for a higher BOC timing sensitivity, the impact on link timing accuracy is less obvious and requires careful analysis. Asymmetric pulse distortions due to fiber nonlinearities and dispersion will shift the BOC zero-crossing relative to the origin, resulting in a timing error for the link pulse arrival time. The timing errors for the round-trip and single-pass pulses are extracted from the zero-crossing positions in the in-loop and out-of-loop BOCs curves, respectively, and plotted in Fig. 4(c). Since we are interested in the timing error at the output of a stabilized link, the round-trip error has been divided by 2 to reflect the half round-trip error; this is because the variable delay is bidirectional and compensates for the round-trip error by imparting half the delay for each of the forward and return paths. The link timing error at the output is therefore the difference in the half round-trip and single-pass errors, i.e. $\Delta t_{LINK} = \frac{1}{2}t_{RT} - t_{SP}$.

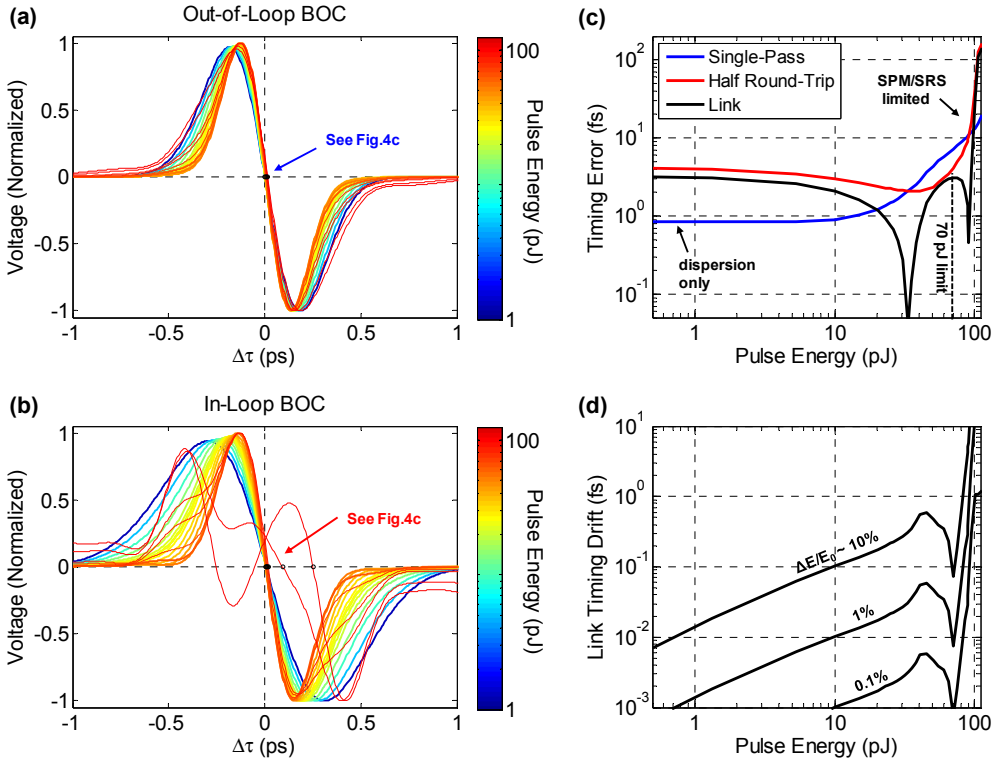

Fig. 4. Simulation results for nonlinear pulse propagation in the 1.2-km PM link and its effects on link timing drift as a function of input pulse energy; (a-b) Normalized output voltage curves for the out-of-loop and in-loop BOC for select pulse energies; (c) single-pass and half round-trip timing error, as extracted from the zero-crossings in the out-of-loop and in-loop BOC output curves, respectively, and link timing error, as defined by the difference in half round-trip and single-pass timing errors, i.e. $|\Delta t_{LINK}| = |\frac{1}{2}t_{RT} - t_{SP}|$ (d) Link timing drift, as extracted from the link timing error curve, corresponding to 0.1%, 1%, and 10% pulse energy fluctuations.

For low pulse energies below 1 pJ, the link error is due to uncompensated 3rd-order dispersion only. Above 1 pJ, intensity-dependent nonlinearities such as SPM and SRS begin to take effect. The round-trip error is typically larger than the single-pass error because the round-trip pulse travels twice as far in the link than the single-pass pulse and experiences more nonlinear distortions. Although the single-pass error increases monotonically, the round-trip error initially decreases due to residual link dispersion and SPM working to reduce

#192815 - $15.00 USD Received 26 Jun 2013; revised 12 Aug 2013; accepted 12 Aug 2013; published 16 Aug 2013

the pulse asymmetry on the return path. These opposing trends add to lower the link error below 3 fs for pulse energies up to 70 pJ. Beyond 90 pJ, complete pulse-splitting and severe distortions due to SPM and SRS cause the link error to increase sharply above tens of fs. These distortions can be identified in the in-loop BOC curves as nonlinear behavior near the zero-crossing (for 100 pJ) or multiple zero-crossings (for 105 pJ). Our experimental set-up was operated with pulse energy of 63 pJ to maximize the BOC timing sensitivity while avoiding the nonlinear threshold at 70 pJ.

It is important to note that timing distribution systems in FELs only require relative timing stability rather than an absolute clock system [11]. The link timing error curve in Fig. 4(c) is a measure of absolute error. When the timing system is initially calibrated for a specific pulse energy operating point, the corresponding link timing error is set as the zero-error reference point. Slow system drifts after the initial calibration may then cause the pulse energy at the link input to fluctuate, causing deviations in the link timing error, or timing drift.

Using the link error curve, the link timing drift due to 0.1%, 1%, and 10% power fluctuations are calculated and plotted in Fig. 4(d). For our experimental set-up with 63-pJ pulse energy and typical ~1% power fluctuations due to beam drifts, we expect the link drift to be only 30 as. This is an order-of-magnitude lower than our experimentally-obtained timing drift of 0.6 fs, indicating that there is much room for improvement. Moreover, since the drifts are caused by intensity-dependent fiber nonlinearities, the pulse energy can be lowered to reduce link drift. Operating at these lower power levels will, however, require integrated BOCs to achieve sufficiently high signal-to-noise ratios to enable sub-fs link stabilization.

5. Conclusion

We have successfully demonstrated long-term stable, sub-femtosecond timing distribution over a 1.2-km PM link for over 16 days with only ~0.6 fs of RMS timing drift and during a 3-day interval only ~0.13 fs drift. This is more than an order-of-magnitude improvement over our previous result, which was limited, at best, to sub-10-fs precision over a few days of operation depending on environmental conditions and was susceptible to large 100-fs delay jumps due to polarization mode dispersion when the fiber was significantly perturbed. Critical to this success was the development and fabrication of a novel dispersion-compensating PM fiber by OFS. The full potential of this link stabilization scheme has yet to be realized; link stability is currently limited by environmental fluctuations in the free-space optics rather than any fundamental limitation in the fiber link itself. Moreover, simulations suggest that stability as low as a few attoseconds can be achieved by operating the link with lower pulse energies to minimize nonlinearity-induced timing errors. Continuing towards sub-100-as stability, ongoing work is focused on switching to an all-fiber implementation to reduce temperature fluctuations and beam drifts and developing an all-integrated, fiber-coupled BOC to greatly reduce the necessary link operating power while simultaneously increasing BOC timing sensitivities for tighter locking of feedback loops.

Acknowledgments

The authors acknowledge financial support by the United States Department of Energy through contract DE-SC0005262, and the Center for Free-Electron Laser Science at Deutsches Elektronen-Synchrotron, Hamburg, a research center of the Helmholtz Association, Germany. M.Y.P. would like to thank Jonathan A. Cox for his preceding work and help in transitioning to the PM fiber link. S.V. acknowledges support by Italian National Civil Authority (ENAC) and University of L'Aquila through Giuliana Tamburro and Ferdinando Filauro scholarships, respectively.

#192815 - $15.00 USD Received 26 Jun 2013; revised 12 Aug 2013; accepted 12 Aug 2013; published 16 Aug 2013